



CHEMISTRY & SUSTAINABILITY

# CHEM **SUS** CHEM

ENERGY & MATERIALS

## Accepted Article

**Title:** Cobalt Complex with Redox Active Imino Bipyridyl Ligand for Electrocatalytic Reduction of Carbon Dioxide to Formate

**Authors:** Fangwei Liu, Jiaojiao Bi, Yuanyuan Sun, Shuping Luo, and Peng Kang

This manuscript has been accepted after peer review and appears as an Accepted Article online prior to editing, proofing, and formal publication of the final Version of Record (VoR). This work is currently citable by using the Digital Object Identifier (DOI) given below. The VoR will be published online in Early View as soon as possible and may be different to this Accepted Article as a result of editing. Readers should obtain the VoR from the journal website shown below when it is published to ensure accuracy of information. The authors are responsible for the content of this Accepted Article.

**To be cited as:** *ChemSusChem* 10.1002/cssc.201800136

**Link to VoR:** <http://dx.doi.org/10.1002/cssc.201800136>

WILEY-VCH

[www.chemsuschem.org](http://www.chemsuschem.org)

A Journal of



## FULL PAPER

## Cobalt Complex with Redox Active Imino Bipyridyl Ligand for Electrocatalytic Reduction of Carbon Dioxide to Formate

Fang-Wei Liu,<sup>[a,c]</sup> Jiaojiao Bi,<sup>[a,c]</sup> Yuanyuan Sun,<sup>[d]</sup> Shuping Luo,<sup>[d]</sup> Peng Kang\*<sup>[a,b,c]</sup>

**Abstract:** An imino bipyridine cobalt (II) complex was developed for electrocatalytic reduction of CO<sub>2</sub> to formate in acetonitrile with ca. 80% faradaic efficiency. For comparison, a symmetric bis-imino pyridine complex showed decreased catalytic activity due to less conjugated system. CV, EPR and IR spectroscopic studies provided mechanistic details and structures of key intermediates. DFT computation confirmed the role of redox active ligand for stabilizing key intermediates through electronic conjugation.

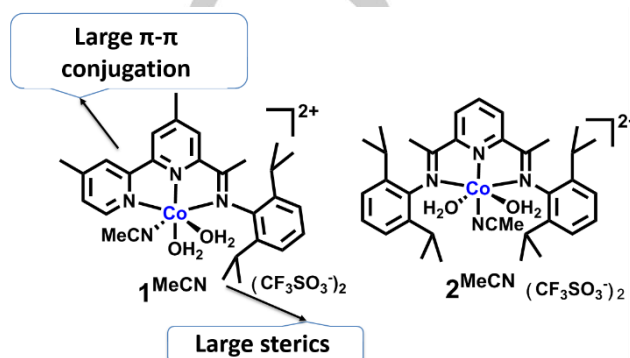
## Introduction

Anthropogenic CO<sub>2</sub> emission has led to observable climate changes. Electrochemical approach could transform industrial CO<sub>2</sub> stream into value-added chemicals.<sup>[1]</sup> Recently, electrocatalytic reduction of CO<sub>2</sub> to carbon monoxide (CO) and formate/formic acid have been investigated,<sup>[2]</sup> and formic acid/formate could serve as hydrogen storage material, deicing agent, drilling completion fluid and precursor to methanol, etc. Efficient and selective electrocatalysts for conversion of CO<sub>2</sub> to formate are desirable.<sup>[3]</sup> Yet, a major challenge is that the reduction of CO<sub>2</sub> is kinetically restrained with multiple electron transfer progresses, and often accompanied with highly competitive hydrogen evolution reaction.

Transition metal complexes are unique catalysts because they can store and transfer multiple electrons, thus circumventing high energy CO<sub>2</sub> radical intermediate. Molecular catalysts using Ru, Ir, Pd and Re have been investigated in converting CO<sub>2</sub> to CO and formate. Catalysts based on earth abundant transition metals,<sup>[4]</sup> such as Fe, Co and Ni, could provide inexpensive materials for large scale use.<sup>[5]</sup> However, these catalysts are quite labile and prone to generate H<sub>2</sub>, causing low selectivity for CO<sub>2</sub> reduction.

Redox active ligands with large π-π conjugation can facilitate electron transfer and storage, thus accelerating electrocatalytic kinetics. Known cobalt complexes with redox active ligands prefer to reduce CO<sub>2</sub> to CO.<sup>[2a-c, 2e, 2f]</sup> Reported transition metal catalysts

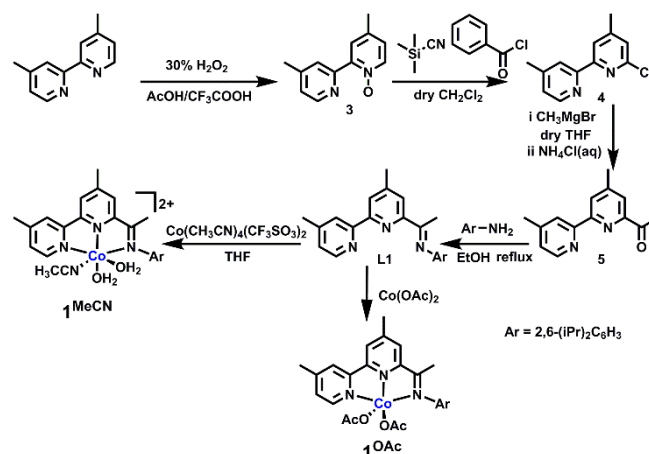
for CO<sub>2</sub>-to-formate conversion are Ir,<sup>[3]</sup> Co,<sup>[2d]</sup> and Ni<sup>[6]</sup> complexes with phosphorus ligands. Little is reported for cobalt complexes that can selectively reduce CO<sub>2</sub> to formate using redox active ligands.



Symmetric bis(imino)pyridine iron and cobalt complexes (ArPDI)MCl<sub>2</sub> were discovered by Brookhart,<sup>[7]</sup> and Gibson,<sup>[8]</sup> and other researchers<sup>[9]</sup> for ethylene polymerization, and recently regain focus in base-metal catalysis.<sup>[5]</sup> However, the above π-conjugated system is not sufficiently large for electrochemical purpose. Herein, a new cobalt complex with large π-conjugated system was developed for CO<sub>2</sub> electroreduction to formate. Compared to bis-terpyridine and bis(imino)pyridine iron and cobalt complexes<sup>[5, 10]</sup>, single tridentate ligand in this study allows more open sites, and large sterics of the diisopropyl moieties can prevent dimerization of the active hydride intermediate,<sup>[11]</sup> which could contribute to increased catalytic reactivity. The electrocatalytic reactivity and mechanism was also explored in detail.

## Results and Discussion

## Synthesis and Physical Properties



[a] F.-W. Liu, J. Bi, Prof. P.Kang  
Key Laboratory of Photochemical Conversion and Optoelectronic Materials, Technical Institute of Physics and Chemistry, Chinese Academy of Sciences, 29 Zhongguancun East Rd, Beijing 100190, China  
E-mail: [pkang@mail.ipc.ac.cn](mailto:pkang@mail.ipc.ac.cn)

[b] Prof. P.Kang  
School of Chemical Engineering and Technology, Tianjin University, 135 Yaguan Rd, Tianjin 300350, China

[c] F.-W. Liu, J. Bi, Prof. P.Kang  
University of Chinese Academy of Sciences, 19A Yuquan Rd, Beijing 100049, China

[d] Y. Sun, Prof. S.Luo  
State Key Laboratory Breeding Base of Green Chemistry-Synthesis Technology, Zhejiang University of Technology, Chaowang Road 18, Hangzhou 310014, China

Supporting information for this article is given via a link at the end of the document

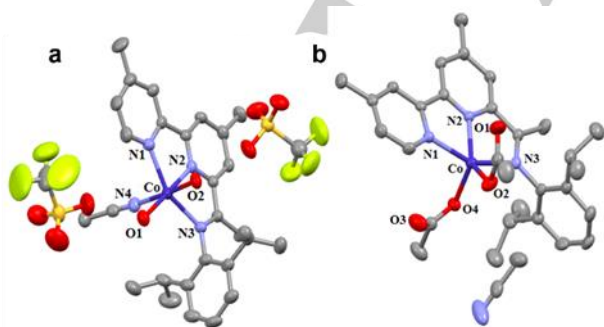
## FULL PAPER

**Scheme 1.** Synthetic route for complexes **1<sup>MeCN</sup>** and **1<sup>OAc</sup>**.

The ligand L1 was synthesized as shown in Scheme 1. 4,4'-dimethyl-2,2'-bipyridine was oxidized by H<sub>2</sub>O<sub>2</sub> to afford *N*-oxidized compound **3**. **3** was cyanated at the 6-position to yield **4**. **4** was then functionalized by Grignard addition with MeMgBr, and subsequent hydrolysis gave the corresponding ketone **5**.<sup>[12]</sup> The bipyridine ligand L1 and symmetrical bis(imino) pyridine ligand L2 was prepared in 85% yield by acid-catalyzed condensation of **5** with 2,6-diisopropylaniline.<sup>[13]</sup>

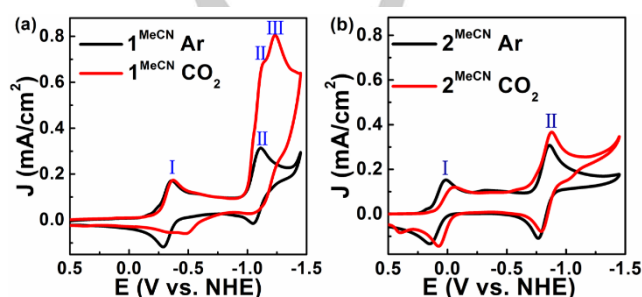
Complexes **1<sup>MeCN</sup>** and **2<sup>MeCN</sup>** were synthesized by treating ligands L1 and L2 with [Co(CH<sub>3</sub>CN)<sub>4</sub>](CF<sub>3</sub>SO<sub>3</sub>)<sub>2</sub> in 1:1 ratio in tetrahydrofuran at room temperature. Complex **1<sup>OAc</sup>** (Scheme 1) was similarly synthesized using Co(OAc)<sub>2</sub> as metal source. Pale-red crystal of **1<sup>MeCN</sup>** suitable for X-ray crystallography was obtained by slow diffusion of diethyl ether into acetonitrile solution at room temperature.<sup>[14]</sup> The crystal structure of **1<sup>MeCN</sup>** (Figure 1a) shows that the cobalt atom was coordinated by three nitrogen atoms of L1 in meridial mode, with one acetonitrile axially coordinated, and two water molecules axially and equatorially coordinated. The water molecules were found in the crystal probably due to adventitious amounts of H<sub>2</sub>O in MeCN. The crystal of **1<sup>OAc</sup>** in Figure 1b shows that two acetate anions coordinated to the cobalt center together with ligand L1. Acetate is a more coordinating ligand and it substituted MeCN in **1<sup>OAc</sup>**. It is interesting that an acetate anion assumed κ-2 coordination, which could serve as a faithful analog for formate coordination.

**1<sup>MeCN</sup>** is a paramagnetic species as observed with broadened NMR resonances. Magnetic susceptibility was measured for **1<sup>MeCN</sup>** using a SQUID magnetometer from 100 to 300 K. Figure S1 shows the magnetic susceptibility  $\chi_M$  and the product  $\chi_M T$  vs temperature. Between 100 and 215 K, the  $\chi_M$  vs  $1/T$  plot (Figure S1; curve for **1<sup>MeCN</sup>**) remained almost constant at 1.53, which corresponds to the spin-only value for  $\mu = 6.21$ ; from 215 to 300 K, the spin-only value changed to  $\mu = 7.36$ . The above results are similar to reported hexacoordinate high-spin Co<sup>II</sup> complexes with N-donor ligands ( $\mu_{\text{eff}} > 4.9\mu_B$ ),<sup>[15]</sup> other than low-spin six-coordinate Co<sup>II</sup> complexes ( $\mu_{\text{eff}} = 1.79\text{--}2.13\mu_B$ ).<sup>[16]</sup> According to the equation,  $\mu = g\sqrt{s(s+1)}$ , and the *g* value of 2.18 for **1<sup>MeCN</sup>** obtained from the solution EPR spectrum (Figure 8a), the electron spin *s* value was calculated to be 3/2 for Co<sup>II</sup>, consistent with high-spin cobalt complexes.



**Figure 1.** Crystal structures of **1<sup>MeCN</sup>** (a) and **1<sup>OAc</sup>** (b). Selected bond lengths [Å] and angles [°] for **1<sup>MeCN</sup>** and **1<sup>OAc</sup>**. **1<sup>MeCN</sup>**: Co-O1 2.030(3), Co-O2 2.129(4), Co-N1 2.179(4), Co-N2 2.052(4), Co-N3 2.191(4), Co-N4 2.113(5). Bond angles:

O1-Co-O2 86.69(15), O1-Co-N1 102.91(15), O1-Co-N2 177.94(16), O1-Co-N3 105.99(15), O1-Co-N4 87.09(16), O2-Co-N1 89.02(15), O2-Co-N3 89.14(15), N1-Co-N3 150.89(15), N2-Co-O2 91.86(15), N2-Co-N1 75.59(16), N2-Co-N3 75.43(15), N2-Co-N4 94.24(17), N4-Co-O2 172.21(16), N4-Co-N1 87.79(17), N4-Co-N3 97.09(16). **1<sup>OAc</sup>**: Co1-O1 2.800, Co1-O2 1.984(3), Co1-O3 3.191, Co1-O4 1.964(3), Co1-N1 2.165(3), Co1-N2 2.046(3), Co1-N3 2.316(3); Bond angles: O2-Co1-N1 100.64(13), O2-Co1-N2 142.29(13), O2-Co1-N3 101.42(13), O4-Co1-O2 104.35(13), O4-Co1-N1 103.73(12), O4-Co1-N2 112.88(13), O4-Co1-N3 89.61(12), N1-Co1-N3 150.41(12), N2-Co1-N1 76.69(12), N2-Co1-N3 73.78(12). Complete crystallography data are collected in SI.

**Electrochemistry under Ar**

**Figure 2.** CVs of **1<sup>MeCN</sup>** (a) and **2<sup>MeCN</sup>** (b) under Ar (black) and CO<sub>2</sub> (red, 1 atm) in MeCN. Conditions: 2 mM complex in 0.1 M *n*Bu<sub>4</sub>NPF<sub>6</sub>/MeCN; glassy carbon working electrode, Pt wire counter electrode, Ag/AgNO<sub>3</sub> reference electrode, scan rate 50 mV/s.

Cyclic voltammograms (CVs) of **1<sup>MeCN</sup>** and **2<sup>MeCN</sup>** were obtained under Ar or 1 atm CO<sub>2</sub> in acetonitrile solutions at room temperature (Figure 2). **1<sup>MeCN</sup>** displayed two reversible redox waves at  $E_{1/2} = -0.33$  V (wave I) and  $-1.08$  V (wave II) vs. NHE under Ar (Figure 2a).<sup>[16-17]</sup> Wave I was electrochemically reversible corresponding to Co<sup>II</sup>/Co<sup>I</sup> redox couple, and wave II was attributed to L1 ligand-centered redox process. **2<sup>MeCN</sup>** also showed two redox waves similar to **1<sup>MeCN</sup>**, but both waves shifted more positively in potential, at  $E_{1/2} = 0.08$  V for wave I and  $-0.80$  V for wave II (Figure 2b). The positive shift in redox potentials was presumably due to decreased electron-donating ability of L2 than L1. The CV of **1<sup>OAc</sup>** under Ar showed two waves at  $E_{1/2} = -0.81$  V for wave I and  $-1.26$  V for wave II (Figure S2), and both shifted more negatively compared to **1<sup>MeCN</sup>**, due to the coordination of OAc<sup>-</sup> to the Co center.

CVs at varied scan rates (10–500 mV/s) under Ar were used to probe the nature of wave I and II (Figure 3a). Both waves were reversible at all scan rates. When normalized for the scan rate ( $i_{\text{cat}}/v^{1/2}$ ) (Figure 3b), the cathodic peak currents ( $i_{\text{p,c}}$ ) of wave I and II varied linearly with the square root of the scan rate ( $v^{1/2}$ ) from 10 to 500 mV s<sup>-1</sup> under Ar (Figure 3c,3d), consistent with diffusional reduction of **1<sup>MeCN</sup>** as shown by the Randles–Sevcik equation (1) and thus these waves were not catalytic under Ar.  $i_d = 0.4463(F^3/RT)^{1/2} n_p^{3/2} AD_{\text{Co}}^{1/2} [\text{Co}] v^{1/2}$  ..... (1) In equation (1), *F* is Faraday's constant, *R* is the universal gas constant (J K<sup>-1</sup> mol<sup>-1</sup>), *n<sub>p</sub>* (=1 for both wave I and II) represents the number of electrons transferred, *T* is the temperature (K), *A* is the electrode area (cm<sup>2</sup>), *D<sub>Co</sub>* represents the diffusion coefficient of the complex (cm<sup>2</sup> s<sup>-1</sup>), and *v* is the scan rate (V s<sup>-1</sup>).<sup>[18]</sup>

## FULL PAPER

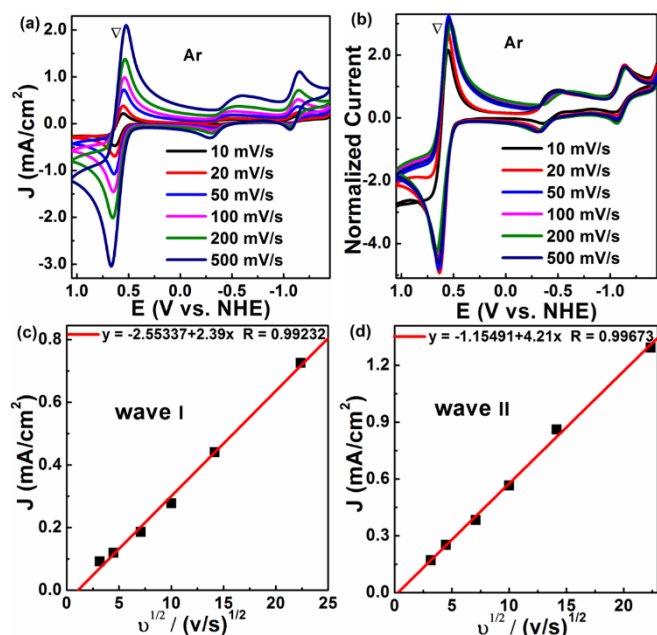


**Figure 3.** Electrochemical study of  $1^{\text{MeCN}}$  at varied scan rates (10–500 mV/s) in MeCN under Ar (0.1 M  $n\text{Bu}_4\text{NPF}_6$ , glassy carbon). (a) CVs of 2 mM  $1^{\text{MeCN}}$  in MeCN under Ar; (b) scan rate normalized ( $i/i_d^{1/2}$ ) CVs from (a); (c) plot of peak current  $i_d$  of wave I under Ar vs the square root of the scan rate ( $v^{1/2}$ ,  $v$  in V/s); (d) plot of peak current  $i_d$  of wave II under Ar vs the square root of the scan rate ( $v^{1/2}$ ,  $v$  in V/s).  $\nabla$ : Ferrocene standard.

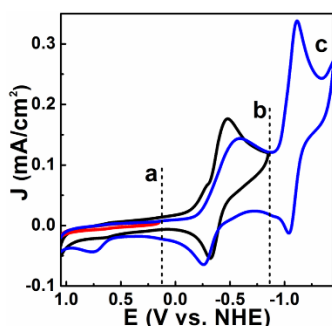


**Figure 4.** CVs of  $1^{\text{MeCN}}$  under Ar starting from 1.05 V to various cathodic limits. To -1.45 V vs. NHE (blue, c); to -0.95 V (black, b); to 0.05 V (red, a). Conditions: 2 mM  $1^{\text{MeCN}}$  in 0.1 M  $n\text{Bu}_4\text{NPF}_6/\text{MeCN}$ ; glassy carbon working electrode, Pt wire counter electrode, Ag/AgNO<sub>3</sub> reference electrode, scan rate 50 mV/s.

CV of  $1^{\text{MeCN}}$  in the presence of 0.1% v/v water showed a new wave at  $E_{p,a} = 0.74$  V vs NHE (Figure 4, trace c), suggesting rapid protonation of the  $\text{Co}^{\text{I}}$  intermediate to generate cobalt hydride species  $[\text{L}1\text{Co}^{\text{I}}\text{H}]^+$  ( $1^{\text{H}}$ ), which was reactive toward  $\text{CO}_2$ .<sup>[19]</sup> No hydride wave appeared after the cathodic scans from 1.05 V to 0.05 V or to -0.95 V vs. NHE (Figure 4, trace a and b) that did not pass wave II, indicating only upon the  $2e^-$  reduction of  $1^{\text{MeCN}}$  could  $1^{\text{H}}$  be formed.

### Electrochemistry under $\text{CO}_2$

When the solution of  $1^{\text{MeCN}}$  was saturated with  $\text{CO}_2$ , wave I kept essentially the same, but the peak current of wave II was catalytically enhanced for ca. 2.2-fold (Figure 2a)<sup>[4d]</sup>. Additionally,

a new wave III appeared at  $E_{p,c} = -1.23$  V vs NHE with current of ca. 2.5-fold of that of wave I. The above observations suggested that catalytic processes occur at waves II and III.  $2^{\text{MeCN}}$  also displayed current enhancement at wave II under  $\text{CO}_2$ , although the catalytic current enhancement was comparably lower, for ca. only 1.2-fold (Figure 2b), suggesting that  $2^{\text{MeCN}}$  was kinetically much less efficient than  $1^{\text{MeCN}}$ .

Under  $\text{CO}_2$  with CV scan rates varied (Figure 5a), wave I remained diffusional in nature, however, wave II became electrocatalytic. When normalized for the scan rate ( $i_{\text{cat}}/v^{1/2}$ ) (Figure 5b), the current of wave II became higher with decreasing scan rate from 500 to 10 mV s<sup>-1</sup>, which pointed to an electrocatalytic process. This was also the case for wave III. Another observation was that the ratio of peak currents of wave II/wave III changed upon variation of the scan rates. At slower scan rates, the current of the wave II increased relative to that of wave III, and vice versa for faster scan rates. We postulated that waves II and III were two separate catalytic processes instead of sequential processes, and it was possible that wave III arose from coordination of generated formate to the Co center as the peak potential was consistent with the wave II of  $1^{\text{OAc}}$  with acetate coordination.

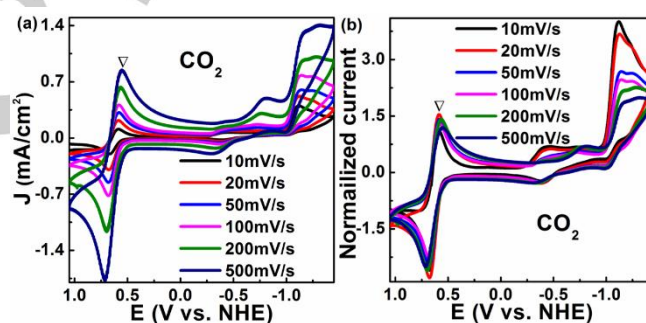


**Figure 5.** Electrochemical study of  $1^{\text{MeCN}}$  at varied scan rates (10–500 mV/s) in MeCN under 1 atm  $\text{CO}_2$  (0.1 M  $n\text{Bu}_4\text{NPF}_6$ , glassy carbon). (a) CVs of 2 mM  $1^{\text{MeCN}}$  at various scan rates (10–500 mV/s) in MeCN under 1 atm  $\text{CO}_2$ ; (b) Scan rate normalized ( $i/i_d^{1/2}$ ) CVs of 2 mM  $1^{\text{MeCN}}$  at various scan rates.  $\nabla$ : Ferrocene standard.

The catalytic kinetics were calculated from CVs at scan rates of 10–50 mV s<sup>-1</sup> using foot-of-wave method reported by Savéant et al. (Figure S3).<sup>[20]</sup> Foot of the wave analysis has been used to evaluate the catalytic efficiency of homogeneous electrocatalysts,<sup>[20]</sup> and was applied to our study, especially when a catalytic current plateau cannot be obtained in the CVs. In equations (2)–(5),  $i_{\text{cat}}$  is given by eqn (3) with  $n_{\text{cat}} = 2$  for  $2e^-$  reduction of  $\text{CO}_2$  to form formate and  $n_p = 1$  for wave II.

$$\text{Rate} = -\frac{d[\text{CO}_2]}{dt} = k_{\text{cat}}[\text{Co}] = k_{\text{CO}_2}[\text{Co}][\text{CO}_2] \quad (2)$$

$$i_{\text{cat}} = (n_{\text{cat}}FA)[\text{Co}](k_{\text{cat}}D_{\text{Co}})^{1/2} = (n_{\text{cat}}FA)[\text{Co}](k_{\text{CO}_2}D_{\text{Co}}[\text{CO}_2])^{1/2} \quad (3)$$

$$\frac{i_{\text{cat}}}{i_d} = 2.242(k_{\text{cat}}RTn_{\text{cat}}^2/n_p^3Fv)^{1/2} \quad (4)$$

$$\frac{i_{\text{cat}}}{i_d} = 2.242(k_{\text{CO}_2}RT[\text{CO}_2]n_{\text{cat}}^2/n_p^3Fv)^{1/2} \quad (5)$$

## FULL PAPER

The observed turnover frequency  $k_{\text{cat}}$  under 1 atm  $\text{CO}_2$  was calculated as  $11.0(1.5) \text{ s}^{-1}$  using CVs at the  $10\text{-}50 \text{ mV s}^{-1}$  scan rates (Figure S3).  $\mathbf{1}^{\text{MeCN}}$  is the second efficient Co catalyst in generating formate, compared to reported P2N2 Co complexes with pendant amines<sup>[2d]</sup>.

Water was used as an exogenous proton source to generate formate. Figure 6a showed CVs of adding water of 0–3% v/v under Ar in MeCN. The wave I of  $\mathbf{1}^{\text{MeCN}}$  shifted more negatively compared to under formally dry conditions, presumably due to water coordination to the Co center to form aqua complexes.<sup>[3a]</sup> Wave II kept essentially unchanged upon adding water, suggesting that  $\mathbf{1}^{\text{MeCN}}$  was not a catalyst toward water reduction to form hydrogen. Still, under  $\text{CO}_2$ , both wave II and wave III increased for 26% and 12% when 3% v/v water was added (Figure 6b), suggesting that moderate water addition can accelerate  $\text{CO}_2$  reduction catalysis. It is possible that water substitutes the coordinated formate increasing the overall catalytic efficiency.

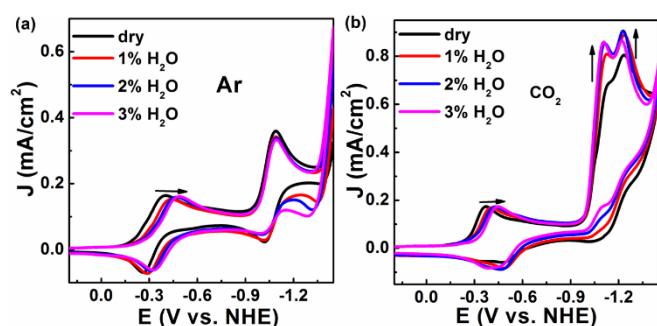


**Figure 6.** CVs of 2 mM  $\mathbf{1}^{\text{MeCN}}$  with 0–3% of water (v/v) added in MeCN under Ar (a) and  $\text{CO}_2$  (b). (0.1 M  $n\text{Bu}_4\text{NPF}_6/\text{MeCN}$ , glassy carbon, 50 mV/s)

## Controlled Potential Electrolysis

Complex  $\mathbf{1}^{\text{MeCN}}$  showed decent stability in electrocatalysis. In Figure 7a, peak currents of wave II and wave III kept nearly constant with 20 cycles of scans.<sup>[21]</sup> Controlled potential electrolysis (CPE) showed fairly stable current density at ca.  $1.5 \text{ mA/cm}^2$  in average for 9 h at  $-1.25 \text{ V}$  vs NHE (Figure 7b). To investigate the  $\text{CO}_2$  reduction products, the headspace of the electrochemical cell was analyzed by gas chromatography and liquid phase by NMR. The  $^1\text{H-NMR}$  spectrum of post electrolysis solutions revealed formate product. The new emerging wave I' of  $\mathbf{1}^{\text{MeCN}}$  (Figure 7a) under  $\text{CO}_2$  was similar to the wave I of  $\mathbf{1}^{\text{OAc}}$  (Figure S2), which suggested that formate product could coordinate to the Co center to form an adduct. With 1% added water, the formate yield was stable at  $>70\%$  over time (Figure 7b). The XPS spectrum of the working electrode after CPE using  $\mathbf{1}^{\text{MeCN}}$  (Figure S4) showed negative response of cobalt element, suggesting that  $\mathbf{1}^{\text{MeCN}}$  did not decompose onto the electrode during the CPE. The NMR spectrum of post CPE solution upon acidic workup showed that the ligand was intact with no observable degradation (Figure S5).

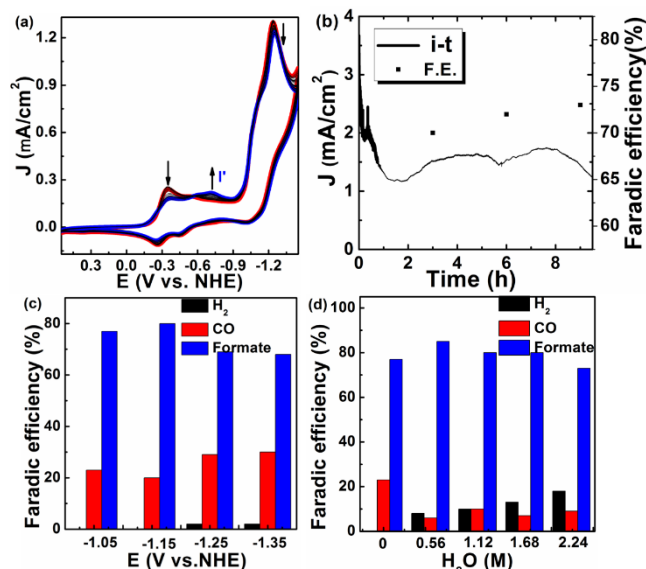


**Figure 7.** Controlled potential electrolyses and product distribution. (a) CVs of  $\mathbf{1}^{\text{MeCN}}$  under 1 atm  $\text{CO}_2$  (20 successive scan cycles). Scan rate =  $100 \text{ mV/s}$ . (b) Time course of CPE and formate efficiencies with 1% added water under  $\text{CO}_2$  in 0.1 M  $n\text{Bu}_4\text{NPF}_6/\text{CH}_3\text{CN}$ . Applied potential,  $-1.25 \text{ V}$  vs. NHE. (c) Faradaic efficiencies and product distribution at various applied potentials. (d) Faradaic efficiencies and product distribution at  $-1.05 \text{ V}$  vs. NHE with different amount of added water. 2 mM  $\mathbf{1}^{\text{MeCN}}$ , glassy carbon working electrodes,  $0.071 \text{ cm}^2$  for CV and  $0.5 \text{ cm}^2$  for CPE, 1 atm  $\text{CO}_2$ , 0.1 M  $n\text{Bu}_4\text{NPF}_6/\text{CH}_3\text{CN}$ , room temperature.

Under formally dry conditions, as the applied potential was more negative from  $-1.05$  to  $-1.35 \text{ V}$ , formate selectivity decreased, and CO selectivity increased from 20% to 30% (Figure 7c). Adding water from 0–4% reduced CO selectivity and increased formate selectivity, but also generated more  $\text{H}_2$  from 0 to 18% (Figure 7d). As much as 80% formate was obtained at  $-1.15 \text{ V}$  in MeCN upon CPE of 5.6 h. Control experiments using  $\text{Co}(\text{CH}_3\text{CN})_4(\text{CF}_3\text{SO}_3)_2$  instead of  $\mathbf{1}^{\text{MeCN}}$  yielded 96%  $\text{H}_2$  and  $< 2\%$  CO, and no formate was found. The average current density was significantly less (ca.  $0.01 \text{ mA cm}^{-2}$ ) than using  $\mathbf{1}^{\text{MeCN}}$  ( $0.36 \text{ mA cm}^{-2}$ ). Those evidences suggested that an intact L1 coordinated cobalt complex was involved in the electrocatalytic process.

## Catalytically Relevant Intermediates

Low-valent Co species were synthesized by preparative electrochemical reduction of  $\mathbf{1}^{\text{MeCN}}$ . By applying constant potential at  $-0.85 \text{ V}$  and  $-1.45 \text{ V}$  respectively, formal  $\text{Co}^{\text{I}}$  species  $\mathbf{1}^{\text{I}}$  and  $\text{Co}^{\text{0}}$  species  $\mathbf{1}^{\text{0}}$  were generated in MeCN under Ar. EPR spectra were measured for the above Co species. The 90 K EPR spectrum of  $\mathbf{1}^{\text{MeCN}}$  in frozen MeCN solution (Figure 8a) showed a rhombic signal at  $g=2.18$  with hyperfine coupling, typical for high-spin square planar  $\text{Co}^{\text{II}}$  complexes ( $d^7$ ,  $s = 3/2$ ). Low-spin ( $s = 1/2$ )  $\text{Co}^{\text{II}}$  complexes could be expected only in the presence of a sufficiently strong ligand field ( $\Delta \geq 15\,000 \text{ cm}^{-1}$ ), which is required for  $^2\text{E}$  ground state,<sup>[12b],[22]</sup> and neither acetonitrile or aqua ligand in  $\mathbf{1}^{\text{MeCN}}$  is strong enough.

## FULL PAPER

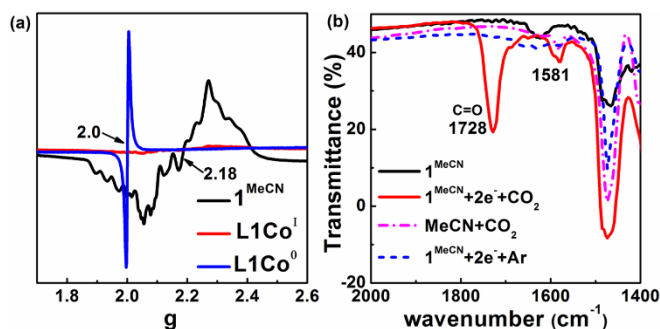
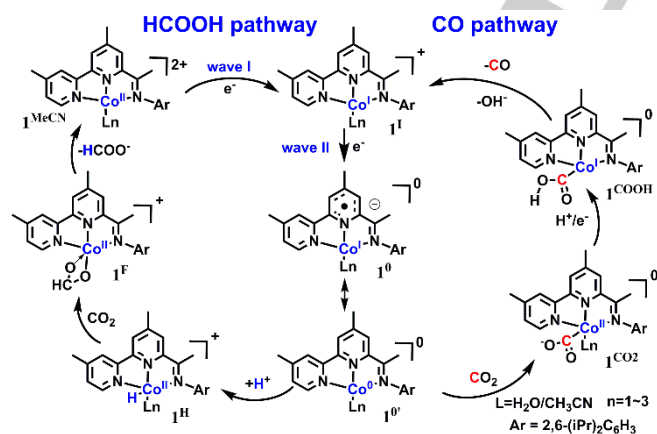


**Figure 8.** Spectra of catalytically relevant Co species. (a) EPR spectra of 10 mM  $1^{\text{MeCN}}$  (black),  $1^{\text{I}}$  (red) and  $1^{\text{O}}$  (blue) in 0.1 M  $n\text{Bu}_4\text{NPF}_6/\text{CH}_3\text{CN}$ . Microwave frequency 9.43 GHz, 10 mW, modulation frequency 100 KHz,  $T = 90$  K. (b) IR-SEC spectra of  $1^{\text{MeCN}}$  (black),  $1^{\text{O}}$  (dash) and  $1^{\text{CO}_2}$  (red) in 0.1 M  $n\text{Bu}_4\text{NPF}_6/\text{CH}_3\text{CN}$ . Electrode, glassy carbon ( $0.071\text{ cm}^2$ ); for reference, an IR spectrum without complex  $1^{\text{MeCN}}$  under  $\text{CO}_2$  is shown in dash dot.

EPR spectrum of  $1^{\text{I}}$  species (Figure 8a) was basically silent with a few residual signals ( $<1\%$ ) of  $1^{\text{MeCN}}$ , suggesting that  $1^{\text{I}}$  is low spin  $d^8$   $\text{Co}^{\text{I}}$  species.<sup>[2e]</sup> The  $1^{\text{O}}$  species showed a free radical signal at  $g=2.00$ , consistent with an organic radical,<sup>[23]</sup> and thus the electronic structure of  $1^{\text{O}}$  should be  $(\text{L}_1^{\cdot-})\text{Co}^{\text{I}}$  species instead of true  $\text{L}_1\text{Co}^{\text{O}}$  species.

The  $1^{\text{O}}$  species reacted with  $\text{CO}_2$  to yield a new intermediate species  $1^{\text{CO}_2}$  under anhydrous conditions. In the infrared spectroscopy (IR) spectra for  $1^{\text{MeCN}}$ ,  $\nu(\text{C}=\text{N})$  bands were located at  $1634\text{ cm}^{-1}$  for imine group.<sup>[13a]</sup> The IR spectrum of  $1^{\text{CO}_2}$  showed feature at  $1728\text{ cm}^{-1}$  (Figure 8b), consistent with  $\text{C}=\text{O}$  vibration of a Co carboxylate  $[\text{LCo}^{\text{II}}(\text{COO}^-)]^{\text{O}}$  species (Scheme 2).<sup>[2e, 4b, 24]</sup>

## DFT Calculations and Proposed Mechanism



**Scheme 2.** Proposed mechanism for electrocatalytic reduction of  $\text{CO}_2$  by  $1^{\text{MeCN}}$ .

Density Functional Theory (DFT) calculations were performed to suggest the electronic configuration of critical intermediates. The optimized structures of  $1^{\text{MeCN}}$ ,  $1^{\text{I}}$ ,  $1^{\text{O}}$  and  $1^{\text{CO}_2}$  species were shown in Figure S6. The HOMO of  $1^{\text{I}}$  mainly consisted of Co  $d_{z^2}$  orbitals, indicating that the first reduction of  $1^{\text{MeCN}}$  occurred at the metal center. The spin density of  $1^{\text{O}}$  mainly distributed over the  $\text{L}_1$

moiety, suggesting that the second reduction was ligand based (Figure S6). In  $1^{\text{CO}_2}$  species, the spin density was redistributed from the reduced ligand to the  $\text{CO}_2$  moiety, suggesting the formation of carboxylate species.<sup>[4d]</sup>

The catalytic mechanism was proposed as shown in Scheme 2.  $1^{\text{MeCN}}$  was electrochemically reduced twice to form  $1^{\text{O}}$  which was catalytically active.  $1^{\text{O}}$  can be protonated by water to form  $\text{Co}^{\text{II}}$  hydride species  $1^{\text{H}}$  (wave II).  $1^{\text{H}}$  was not sufficiently reactive with water to form  $\text{H}_2$  as shown in CVs, yet sufficiently hydridic to insert  $\text{CO}_2$  to form formate adduct  $1^{\text{F}}$ . The formate dissociated from the Co center with the aid of water to regenerate  $1^{\text{MeCN}}$ , completing the formate pathway.

Alternatively, under formally dry conditions,  $1^{\text{O}}$  could nucleophilically attack  $\text{CO}_2$  to form  $1^{\text{CO}_2}$ , introducing the CO pathway in Scheme 2. The formation of  $1^{\text{CO}_2}$  enabled a second reduction at the metal center or the ligand at the same potential followed by proton transfer to form a transient  $[\text{LCo}^{\text{I}}(\text{COOH})]^{\text{O}}$   $1^{\text{COOH}}$  species (Scheme 2). The decomposition of  $1^{\text{COOH}}$  presumably yielded the CO product. However, in CPE experiments with water added, this became a comparably minor pathway as  $1^{\text{O}}$  was rapidly protonated to form  $1^{\text{H}}$ .

In the proposed mechanism, the CO and formate pathways share the same  $\text{Co}^{\text{O}}$  species  $1^{\text{O}}$ , and redox active imino bipyridial ligand is effective in delocalizing electron density from the Co center to the ligand, thus making the Co center less electron rich. Compared to phosphine based Co complexes,  $1^{\text{H}}$  species is not sufficiently hydridic, which reduces the chance for undesired  $\text{H}_2$  evolution in the presence of added water and enhances the formate selectivity.<sup>[19]</sup>

## Conclusions

The Co complex of redox active imino bipyridial ligand is efficient in electrochemical reduction of  $\text{CO}_2$  to formate in acetonitrile with 80% selectivity. The Co complex does not catalyze water reduction to generate  $\text{H}_2$ . Adding water can promote the formation of formate and reduce CO formation, although leading to slightly more  $\text{H}_2$  evolution. Catalytically relevant Co intermediate species were synthesized, and based on these intermediates the catalytic mechanism was proposed. The function of redox active ligand is critical in contributing the  $\text{CO}_2$  reduction efficiency and selectivity, and translation of the catalytic reactivity into aqueous phase is currently underway.

## Experimental Section

## Materials and Methods

All chemicals were purchased from commercial sources if not mentioned otherwise. 4,4'-dimethyl-2,2'-bipyridine was purchased from Acros. Compounds  $3$ <sup>[25]</sup>,  $4$ <sup>[12a]</sup>,  $5$ <sup>[12]</sup>,  $\text{L}2$ <sup>[26]</sup> and  $\text{Co}(\text{CH}_3\text{CN})_4(\text{CF}_3\text{SO}_3)_2$ <sup>[27]</sup> were synthesized according to published procedures. Particularly, the synthesis of  $\text{Co}(\text{CH}_3\text{CN})_4(\text{CF}_3\text{SO}_3)_2$  is similar to  $\text{Fe}(\text{CH}_3\text{CN})_4(\text{OTf})_2$  in the reference.<sup>[27]</sup> Acetonitrile was of HPLC grade and further purified by a solvent purification system. Deionized water was further purified by using a Master-S15 UV Water Purification system.

## FULL PAPER

NMR spectra were recorded with a Bruker Advance 400 spectrophotometer. High-resolution mass spectrometry experiments were performed with a Bruker Daltonics Apex IV spectrometer. Infrared-spectrum was recorded by Varian 3100 FT-IR. Electron paramagnetic resonance spectra were obtained on a Varian-E-500 EPR spectrometer. The spectra were recorded for solutions of the complexes in CH<sub>3</sub>CN solvent at liquid nitrogen temperature (77 K). Crystal structures were solved with direct methods and refined with a full-matrix least-squares technique, using the SHELXS software package. Mercury (CSD software) was used for crystal structure visualization. The Co elements on the glassy carbon electrode were investigated using X-ray photoelectron spectroscopy (XPS; ESCALab250Xi, Thermo Scientific).

Electrochemical experiments were performed using a CHI 660E potentiostat (CH Instruments, Inc.). The three-electrode system consisted of a glassy carbon working electrode, a coiled Pt wire counter electrode, and a Ag/AgNO<sub>3</sub> reference electrode (CHI, 10 mM AgNO<sub>3</sub>, 0.1 M nBu<sub>4</sub>NPF<sub>6</sub> in acetonitrile, 0.55 V vs NHE) in an airtight, glass frit-separated two compartment cell. Prior to each measurement, glassy carbon electrode (CHI, 7.1 mm<sup>2</sup>) was polished with 0.05-μm alumina slurry to obtain a mirror surface and it was then sonicated and thoroughly rinsed with ultrapure water and acetone. For cyclic voltammogram experiments, working and counter electrodes were separated from the reference electrode. For controlled potential electrolyses, reference and counter electrodes were separated from the working electrode. Ferrocene was added at the end of the experiment and the potential was converted relative to NHE by adding 0.55V following the literature.<sup>[28]</sup> Gaseous product was analyzed using an SRI 8610C GC with a molecular sieve column and a HID detector. The concentrations of H<sub>2</sub> and CO were obtained from GC calibrated using external gas standard. The concentration of formate was obtained by <sup>1</sup>H-NMR using DMF as internal standard.

## Syntheses

The synthesis of **1**<sup>MeCN</sup> and **2**<sup>MeCN</sup> is outlined in Scheme 1. The details are as follows.

**Preparation of 5**<sup>[17]</sup>: To a solution of **4** (1.05 g, 5.0 mmol) in dry THF (50 mL) was added dropwise MeMgBr (3.0 M in Et<sub>2</sub>O, 0.85 mL, 2.5 equiv, 12.5 mmol) at -15 °C. The reaction mixture was further stirred for 1 h at -15 °C and then for 2 h at rt to give an orange-red solution. Slow addition of a saturated NH<sub>4</sub>Cl solution (30 mL) was followed by phase separation. The aqueous phase was extracted with THF (50 mL) and then CH<sub>2</sub>Cl<sub>2</sub> (50 mL). The combined organic phases were washed with saturated NaCl solution (50 mL) and then dried over MgSO<sub>4</sub>. Evaporation of the filtrate in vacuo left a reddish oil. Extraction with hexane (3 × 100 mL) and removal of the solvent in vacuo yielded **5** as an off-white solid (735 mg, 3.25 mmol, 65.0%). <sup>1</sup>H NMR (400 MHz, CDCl<sub>3</sub>): δ 8.55 (d, J = 5.0 Hz, 1H), 8.44 (s, 1H), 8.33 (s, 1H), 7.88 (s, 1H), 7.17 (d, J = 4.9 Hz, 1H), 2.83 (s, 3H), 2.49 (d, J = 4.3 Hz, 6H).

**Preparation of L1**<sup>[29]</sup>: **5** (226 mg, 1.00 mmol) was dissolved in ethanol (10 mL), and ten drops of acetic acid was added to the solution, and then 2,6-diisopropylaniline (0.38 mL, 2.00 mmol) was introduced. The solution was heated to reflux and stirred for 72 h. After cooling to room temperature, the solvent was removed with reduced pressure. The precipitate was resolved in chloroform and washed with saturated aqueous NaHCO<sub>3</sub>, brine and dried over Na<sub>2</sub>SO<sub>4</sub>. After the solvent was removed by rotary

evaporation, further purification was carried out by column chromatography using CH<sub>2</sub>Cl<sub>2</sub> / CH<sub>3</sub>OH (100: 3, v / v) as eluent to afford 308 mg of product **L1**. Yield: 80 %. <sup>1</sup>H NMR (400 MHz, CDCl<sub>3</sub>): δ 8.57 (d, J = 4.9 Hz, 1H, Py-CH), 8.38 (d, J = 6.0 Hz, 2H, Py-CH), 8.24 (s, 1H, Py-CH), 7.20 (d, J = 7.6 Hz, 2H, Ar-CH), 7.18 – 7.10 (t, 1H, Ar-CH), 7.15 (d, J = 4.0 Hz, 1H, Py-CH) 2.91 – 2.74 (m, 2H, CH<sub>3</sub>CHCH<sub>3</sub>), 2.48-2.55 (d, 6H, CH<sub>3</sub>-Py), 2.36 (s, 3H, CH<sub>3</sub>C=N), 1.24 – 1.12 (m, 12H, CH<sub>3</sub>CHCH<sub>3</sub>). <sup>13</sup>C NMR (400 MHz, CDCl<sub>3</sub>): δ 167.5 (Cq, s, C=N-Ar), 156.1 (Cq, s, Py-C), 155.7 (Cq, s, Py-C), 155.1 (Cq, s, Py-C), 149.1 (CH, s, Py-C), 148.7 (Cq, s, Py-C), 148.1 (Cq, s, Py-C), 146.7 (Cq, s, Ar-C-N), 136.1 (Cq, s, Ar-C), 124.9 (CH, s, Py-C), 123.7 (Cq, s, Ar-C), 123.2 (CH, s, Py-C), 123.1 (CH, s, Ar-C), 122.1 (CH, s, Ar-C), 121.9 (CH, s, Py-C), 28.4 (CH, s, CH<sub>3</sub>CHCH<sub>3</sub>), 23.2-23.4 (CH, d, CH<sub>3</sub>CHCH<sub>3</sub>), 21.5 (CH, s, CH<sub>3</sub>-Py), 17.6 (CH, s, CH<sub>3</sub>-C=N). HR-ESI-MS: m/z calcd for [M]<sup>+</sup> C<sub>26</sub>H<sub>32</sub>N<sub>3</sub>: 386.259074; found: 386.259151, error: 0.2 ppm; calcd for [M+Na]<sup>+</sup> C<sub>26</sub>H<sub>31</sub>N<sub>3</sub>Na: 408.241019; found: 408.240803, error: 0.5 ppm.

**Preparation of 1**<sup>MeCN</sup>: To 20 mL dry THF solution of **L1** (77 mg, 0.20 mmol) was added Co(CH<sub>3</sub>CN)<sub>4</sub>(CF<sub>3</sub>SO<sub>3</sub>)<sub>2</sub> (104 mg, 0.20 mmol) and stirred at room temperature overnight. The solvent was removed with reduced pressure to afford 92 mg of yellow product. Yield: 95 %. <sup>1</sup>H NMR (400 MHz, CD<sub>3</sub>CN): δ 8.51 (s, 3H), 5.97 (s, 1H), 5.73 (s, 3H), -1.33 (s, 6H), -2.13 (s, 3H), -8.96 (s, 6H). HR-ESI-MS: m/z calcd for 1/2[M-CH<sub>3</sub>CN-2H<sub>2</sub>O]<sup>2+</sup> C<sub>26</sub>H<sub>31</sub>CoN<sub>3</sub>: 222.091948; found: 222.091992, error: 0.2 ppm; calcd for 1/2[M-2H<sub>2</sub>O]<sup>2+</sup> C<sub>28</sub>H<sub>34</sub>CoN<sub>4</sub>: 242.605222; found: 242.605218, error: 0.0 ppm; calcd for 1/2[M+2H]<sup>2+</sup> C<sub>28</sub>H<sub>38</sub>CoN<sub>4</sub>O<sub>2</sub>: 261.613048; found: 261.613047, error: -0.0 ppm.

**Preparation of 2**<sup>MeCN</sup>: **2**<sup>MeCN</sup> were synthesized according to the synthesis of **1**<sup>MeCN</sup>.

**Computational Details.** All calculations were carried out with the unrestricted B3LYP hybrid density functional method.<sup>[30]</sup> Geometry optimizations have been carried out using B3LYP/6-31G\*/gas phase in Gaussian 09 program package (Revision g09w). Frequency calculations on the optimized structures confirm the absence of imaginary frequencies. The Cartesian coordinates of the optimized structures are available in SI.

## Acknowledgements

This work was financially supported by National Key Research and Development Program of China (2016YFB0600901), and Key Research Program of the Chinese Academy of Sciences (ZDRW-ZS-2016-3). Thanks for the computing service of CNGrid and ScGrid based on the SCE software.<sup>[31]</sup>

**Keywords:** Cobalt Complexes, Electrocatalytic Reduction of Carbon Dioxide, Formate, Redox Active Ligand

- [1] a) B. Kumar, M. Llorente, J. Froehlich, T. Dang, A. Sathrum, C. P. Kubiak, *Annu. Rev. Phys. Chem.* **2012**, *63*, 541-569; b) H. Takeda, C. Cometto, O. Ishitani, M. Robert, *ACS Catal.* **2016**, *7*, 70-88.
- [2] a) Z. Guo, S. Cheng, C. Cometto, E. Anxolabéhère-Mallart, S.-M. Ng, C.-C. Ko, G. Liu, L. Chen, M. Robert, T.-C. Lau, *J. Am. Chem. Soc.* **2016**, *138*, 9413-9416; b) A. Chapovetsky, T. H. Do, R. Haiges, M. K. Takase, S. C. Marinescu, *J. Am. Chem. Soc.* **2016**, *138*, 5765-5768; c) D.

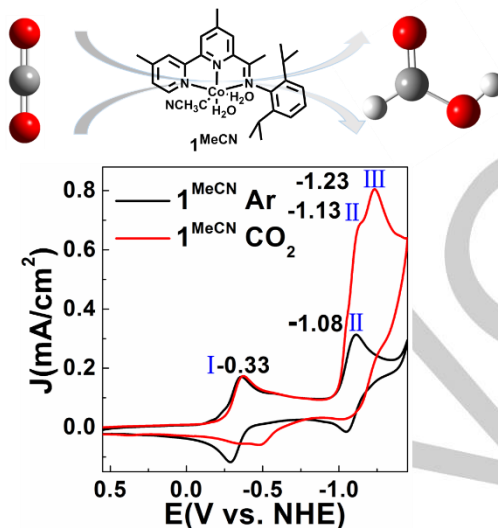
## FULL PAPER

- C. Lacy, C. C. McCrory, J. C. Peters, *Inorg. Chem.* **2014**, *53*, 4980-4988; d) S. Roy, B. Sharma, J. Pecaut, P. Simon, M. Fontecave, P. D. Tran, E. Derat, V. Artero, *J. Am. Chem. Soc.* **2017**, *139*, 3685-3696; e) M. Zhang, M. El-Roz, H. Frei, J. Mendoza-Cortes, M. Head-Gordon, D. C. Lacy, J. C. Peters, *The Journal of Physical Chemistry C* **2015**, *119*, 4645-4654; f) H. Sheng, H. Frei, *J. Am. Chem. Soc.* **2016**, *138*, 9959-9967.
- [3] a) P. Kang, C. Cheng, Z. Chen, C. K. Schauer, T. J. Meyer, M. Brookhart, *J. Am. Chem. Soc.* **2012**, *134*, 5500-5503; b) P. Kang, S. Zhang, T. J. Meyer, M. Brookhart, *Angew. Chem. Int. Ed.* **2014**, *53*, 8709-8713.
- [4] a) P. L. Cheung, C. W. Machan, A. Y. Malkhasian, J. Agarwal, C. P. Kubiak, *Inorg. Chem.* **2016**, *55*, 3192-3198; b) C. W. Machan, J. Yin, S. A. Chabolla, M. K. Gilson, C. P. Kubiak, *J. Am. Chem. Soc.* **2016**, *138*, 8184-8193; c) M. D. Sampson, C. P. Kubiak, *J. Am. Chem. Soc.* **2016**, *138*, 1386-1393; d) B. A. Johnson, S. Maji, H. Agarwala, T. A. White, E. Mijangos, S. Ott, *Angew. Chem. Int. Ed.* **2016**, *128*, 1857-1861.
- [5] P. J. Chirik, *Acc. Chem. Res.* **2015**, *48*, 1687-1695.
- [6] C. S. Seu, A. M. Appel, M. D. Doud, D. L. DuBois, C. P. Kubiak, *Energy Environ. Sci.* **2012**, *5*, 6480-6490.
- [7] S. D. Ittel, L. K. Johnson, M. Brookhart, *Chem. Rev.* **2000**, *100*, 1169-1204.
- [8] a) G. J. Britovsek, S. P. Baugh, O. Hoarau, V. C. Gibson, D. F. Wass, A. J. White, D. J. Williams, *Inorg. Chim. Acta* **2003**, *345*, 279-291; b) G. J. Britovsek, M. Bruce, V. C. Gibson, B. S. Kimberley, P. J. Maddox, S. Mastroianni, S. J. McTavish, C. Redshaw, G. A. Solan, S. Strömberg, *J. Am. Chem. Soc.* **1999**, *121*, 8728-8740.
- [9] H. Kazumasa, K. Kouji, N. Hiroshi, *Bull. Chem. Soc. Jpn.* **2016**, *89*, 394-404.
- [10] a) S. Aroua, T. K. Todorova, P. Hommes, L.-M. Chamoreau, H.-U. Reissig, V. Mougél, M. Fontecave, *Inorg. Chem.* **2017**, *56*, 5930-5940; b) S. M. Fatur, S. G. Shepard, R. F. Higgins, M. P. Shores, N. H. Damrauer, *J. Am. Chem. Soc.* **2017**, *139*, 4493-4505.
- [11] D. Zhu, I. Korobkov, P. H. M. Budzelaar, *Organometallics* **2012**, *31*, 3958-3971.
- [12] a) J. I. van der Vlugt, S. Demeshko, S. Dechert, F. Meyer, *Inorg. Chem.* **2008**, *47*, 1576-1585; b) B. Schneider, S. Demeshko, S. Neudeck, S. Dechert, F. Meyer, *Inorg. Chem.* **2013**, *52*, 13230-13237.
- [13] a) Y. D. M. Champouret, J.-D. Marechal, R. K. Chaggar, J. Fawcett, K. Singh, F. Maseras, G. A. Solan, *New J. Chem.* **2007**, *31*, 75-85; b) V. Radkov, T. Roisnel, A. Trifonov, J.-F. Carpentier, E. Kirillov, *J. Am. Chem. Soc.* **2016**, *138*, 4350-4353; c) C. Bianchini, D. Gatteschi, G. Giambastiani, I. Guerrero Rios, A. Ienco, F. Laschi, C. Mealli, A. Meli, L. Sorace, A. Toti, F. Vizza, *Organometallics* **2007**, *26*, 726-739.
- [14] a) W.-H. Sun, S. Jie, S. Zhang, W. Zhang, Y. Song, H. Ma, J. Chen, K. Wedeking, R. Fröhlich, *Organometallics* **2006**, *25*, 666-677; b) M. Käls, J. Hohenberger, M. Adelhardt, E. M. Zolnhofer, S. Mossin, F. W. Heinemann, J. Sutter, K. Meyer, *Inorg. Chem.* **2014**, *53*, 2460-2470.
- [15] D. D. S. G. S. Wilson, and R. S. Glass, *Inorg. Chem.* **1985**, *25*, 3827-3829.
- [16] A. K. Singh, R. Mukherjee, *Dalton Trans.* **2008**, 260-270.
- [17] a) S. Seka, O. Buriez, J. Périchon, *Chem. Eur. J.* **2003**, *9*, 3597-3603; b) S. Heider, H. Petzold, J. M. Speck, T. Ruffer, D. Schaarschmidt, *Zeitschrift für anorganische und allgemeine Chemie* **2014**, *640*, 1360-1367.
- [18] P. Kang, T. J. Meyer, M. Brookhart, *Chem. Sci.* **2013**, *4*, 3497.
- [19] a) E. S. Wiedner, M. B. Chambers, C. L. Pitman, R. M. Bullock, A. J. M. Miller, A. M. Appel, *Chem. Rev.* **2016**, *116*, 8655-8692; b) Z. M. Heiden, A. P. Lathem, *Organometallics* **2015**, *34*, 1818-1827.
- [20] a) E. S. Rountree, B. D. McCarthy, T. T. Eisenhart, J. L. Dempsey, *Inorg. Chem.* **2014**, *53*, 9983-10002; b) C. Costentin, J.-M. Savéant, *ChemElectroChem* **2014**, *1*, 1226-1236.
- [21] a) S. Zhang, P. Kang, M. Bakir, A. M. Lapides, C. J. Dares, T. J. Meyer, *Proc. Natl. Acad. Sci. USA* **2015**, *112*, 15809-15814; b) Z. Chen, J. J. Concepcion, M. K. Brennaman, P. Kang, M. R. Norris, P. G. Hoertz, T. J. Meyer, *Proc. Natl. Acad. Sci. USA* **2012**, *109*, 15606-15611.
- [22] C. C. Hojilla Atienza, C. Milsman, E. Lobkovsky, P. J. Chirik, *Angew. Chem. Int. Ed.* **2011**, *50*, 8143-8147.
- [23] a) S. Pramanik, S. Dutta, S. Roy, S. Dinda, T. Ghorui, A. Kumar Mitra, K. Pramanik, S. Ganguly, *New J. Chem.* **2017**, *41*, 4157-4164; b) P. Sarkar, M. K. Mondal, A. Sarmah, S. Maity, C. Mukherjee, *Inorg. Chem.* **2017**, *56*, 8068-8077.
- [24] a) J. Hawecker, J. M. Lehn, R. Ziessel, *Helve. chim. acta* **1986**, *69*, 1990-2012; b) F. P. Johnson, M. W. George, F. Hartl, J. J. Turner, *Organometallics* **1996**, *15*, 3374-3387; c) F. Franco, C. Cometto, L. Nencini, C. Barolo, F. Sordello, C. Minero, J. Fiedler, M. Robert, R. Gobetto, C. Nervi, *Chem. Eur. J.* **2017**, *23*, 4782-4793; d) S. C. Cheng, C. A. Blaine, M. G. Hill, K. R. Mann, *Inorg. Chem.* **1996**, *35*, 7704-7708; e) F. Blasco, L. Perelló, J. Latorre, J. Borrás, S. García-Granda, *Inorg. Biochem.* **1996**, *61*, 143-154.
- [25] M. Mettry, M. P. Moehlig, R. J. Hooley, *Org. Lett.* **2015**, *17*, 1497-1500.
- [26] A. P. Singh, H. W. Roesky, E. Carl, D. Stalke, J.-P. Demers, A. Lange, *J. Am. Chem. Soc.* **2012**, *134*, 4998-5003.
- [27] K. S. Hagen, *Inorg. Chem.* **2000**, *39*, 5867-5869.
- [28] V. V. Pavlishchuk, A. W. Addison, *Inorg. Chim. Acta* **2000**, *298*, 97-102.
- [29] J. D. Pelletier, Y. D. Champouret, J. Cadarso, L. Clowes, M. Gañete, K. Singh, V. Thanarajasingham, G. A. Solan, *Organometallics* **2006**, *25*, 4114-4123.
- [30] C. Lee, W. Yang, R. G. Parr, *Physical Review B* **1988**, *37*, 785-789.
- [31] a) H. Xiao, H. Wu, X. Chi, Springer Berlin Heidelberg, Berlin, Heidelberg, **2009**, pp. 35-42; b) P. Vicat-Blanc Primet, T. Kudoh, J. Mambretti, Springer Berlin Heidelberg, Berlin, Heidelberg, **2009**, pp. E1-E1.

Entry for the Table of Contents (Please choose one layout)

## FULL PAPER

An imino bipyridine cobalt (II) complex was developed for electrocatalytic reduction of CO<sub>2</sub> to formate in acetonitrile with 80% efficiency. CV, EPR and IR spectroscopic studies have provided mechanistic details and structures of key intermediates. DFT computation confirmed the beneficial role of large  $\pi$ - $\pi$  conjugate groups.



Fang-Wei Liu, Jiaojiao Bi,  
Yuanyuan Sun, Shuping Luo,  
Peng Kang\*

Page No. – Page No.

Cobalt Complex with Redox  
Active Imino Bipyridyl Ligand  
for Electrocatalytic Reduction  
of Carbon Dioxide to Formate